

# Guidance, Navigation and Control of Fixed-Wing Unmanned Aerial Vehicles

Tor A. Johansen and Thor I. Fossen

Center for Autonomous Marine Operations and Systems (NTNU-AMOS),  
Department of Engineering Cybernetics, Norwegian University of Science and  
Technology, Trondheim  
tor.arne.johansen@ntnu.no, thor.fossen@ntnu.no

## Synonyms

We will use the term Unmanned Aerial Vehicle (UAV). It is closely related to Unmanned Aerial Systems (UAS), which emphasize that the vehicle needs to be operated as part of a larger system that includes ground control, handling systems, and systems for communication and navigation. It is also closely related to Remotely Piloted Aircraft Systems (RPAS), which is the term used by regulators to emphasize that the system is actually not unmanned but requires a remote pilot in command. UAV's are also known as aerial robots and drones.

## Definitions

The topic of this chapter is the guidance, navigation and control (GNC) of fixed-wing UAVs. Fixed-wing aircraft are characterized by the use of forward speed to generate a lift force that compensates for the weight of the aircraft, as well as maneuvering capabilities through control surfaces that can generate desired control moments by changing actuator positions. We consider fixed-wing UAVs that generate their forward speed by a propulsion system, typically by propellers driven by electric motors or liquid fuel engines. In other words, we do not consider rotary wing UAVs such as multi-copters/multi-rotors and helicopters. Also, we do not explicitly consider hybrids or gliders, although much of the flight control principles are applicable for several of their operation modes.

---

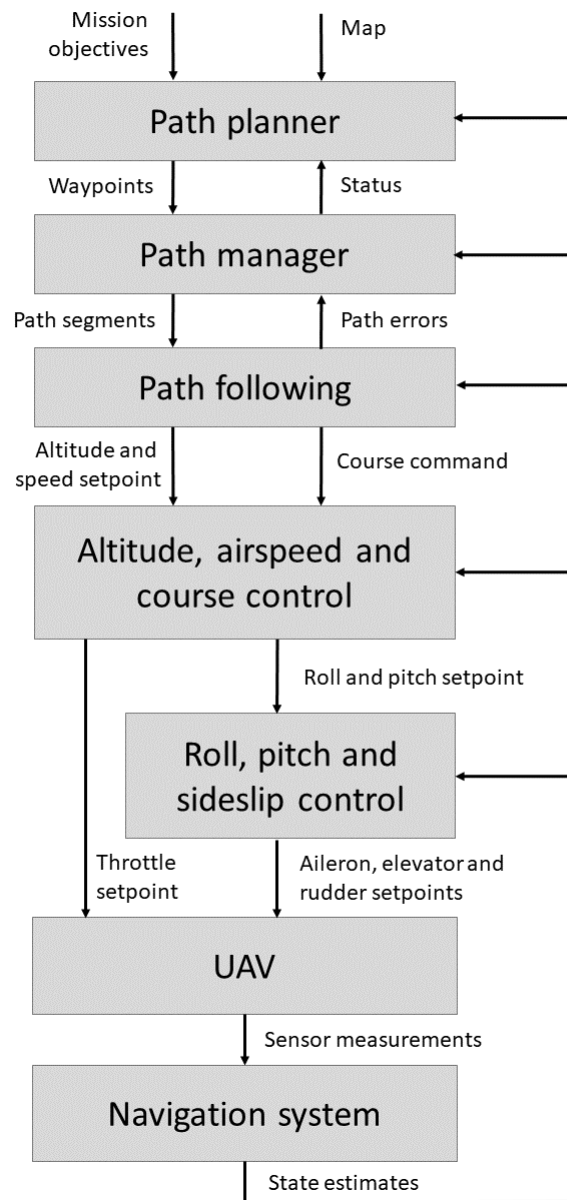
This work is supported by the Research Council of Norway through the Centers of Excellence funding scheme, grant 223254.

## Overview

Flight management systems for UAV usually involves several control modes. In manual control mode the pilot controls the control surfaces and engine throttle directly, while in automatic mode they are controlled by the flight control computer according to a pre-programmed flight plan. There are also mixed modes where low-level control is done automatically, while higher-level control is done manually. Moreover, there may be autonomous flight modes where the flight plan is updated on-the-fly by the control system.

A fully automatic flight control architecture is illustrated with a block diagram in Figure 1. The architecture is typical for automatic flight control systems implemented in commercial UAV flight management systems and autopilots, and the structures presented in textbooks such as Beard and McLain (2012). A summary of the architecture is made by describing each of its main modules:

- **Path planner:** The path planner or guidance system provides a sequence of way-points based on mission objectives such as mapping and surveillance, and constraints such as terrain, weather, air space and fuel. This is often done manually by the pilot that directly specifies the way point sequence, although there exist numerous algorithms that can make the plan automatically. Plans can change during flight as re-planning can be necessary due to new information becoming available.
- **Path manager:** The path manager specifies how the UAV should travel between the way-points. This is usually an automatic function that considers the specifications of the UAV in order to generate a path consisting of segments of lines and circles that are compatible with the UAV's turn and climb capabilities.
- **Path following:** The path-following control (also known as guidance) will specify changes in course, altitude and airspeed necessary to follow the specified path, typically represented as a sequence of line and circle segments. This will correct for track errors if the UAV is deviating from the desired path due to path updates, winds and other disturbances.
- **Altitude, airspeed and course control:** In the longitudinal dimension the speed is usually controlled to its reference by commanding the engine throttle, and the altitude is usually controlled to its reference by commanding the elevators. In some cases it might be beneficial to combine these controllers into a coupled structure since they are closely coupled by the fact that the lift and drag force are strongly dependent on airspeed. In the lateral dimension the course is usually controlled by a coordinated bank-to-turn maneuver by controlling the ailerons to achieve a desired roll angle.
- **Roll, pitch and side-slip control:** Low-level controllers provide control of the UAV's attitude. This provides tracking of references from the pilot or higher-level control, rejects disturbances due to both steady and turbulent winds, and is sometimes necessary to stabilize unstable dynamics of the aircraft.
- **UAV:** The main interface to the UAV is to the propulsion system (throttle command) and control surfaces that are actuated by DC servo motors. The com-

**Fig. 1** Flight control structure

mon control surfaces are ailerons, elevators, rudder and flaps. Control forces and moments can also be generated by other control surfaces or differential thrust provided by two or more propellers. In addition comes the sensors used by the navigation system, described next.

- **Navigation system:** The basic sensors required by the flight control system are GNSS (global navigation satellite system) for position and velocity over ground, pitot-static tube for airspeed, and inertial sensors for linear acceleration in 3D and angular rates (gyros) in 3D. In addition, a barometric pressure altimeter is necessary in some cases when GNSS may not be sufficiently accurate in the vertical direction, and laser or radar altimeters might be useful for automatic landing. Heading sensors such as magnetometer, camera or two-antenna GNSS are sometimes used, but generally not necessary for flight control, except in special cases such as automatic takeoff. Accurate heading is, however, usually important for geo-referencing of the payload data such as images.

Mixed control modes allow the pilot to benefit from automatic low-level stabilization and control through interfaces that typically allows the pilot to command velocities or hold airspeed, altitude, flight plan, course, pitch or roll angle. Autonomous control based on e.g. camera sensors or special modes for takeoff and landing requires special attention and may replace the path planning, management and following blocks in Figure 1 with other functions and interfaces. In the next section we will provide an overview of the most common approaches to the navigation and lower-level control modules. We will not consider the path planner and path manager but refer to other literature such as Beard and McLain (2012); Tsourdos et al (2010); Alexis et al (2019); Maza and Ollero (2019).

## Key Research Findings

Most fixed-wing UAVs operate in restricted flight envelopes where the lateral and longitudinal dynamics are only weakly coupled. Fixed-wing UAVs are slender bodies and the forward/vertical velocities are much larger than the transverse velocity. This suggests that the lateral and longitudinal control designs can be decoupled. Couplings due to special arrangements of control surfaces, such as elevons and V-tails, can be decoupled by inverting simple mathematical models of the forces and moments, or a control allocation logic can be implemented. We will therefore only consider decoupled dynamics here, and refer to Johansen and Fossen (2013) for details about redundant and coupled control surfaces.

### *Lateral guidance and control*

The decoupled lateral control loops are:

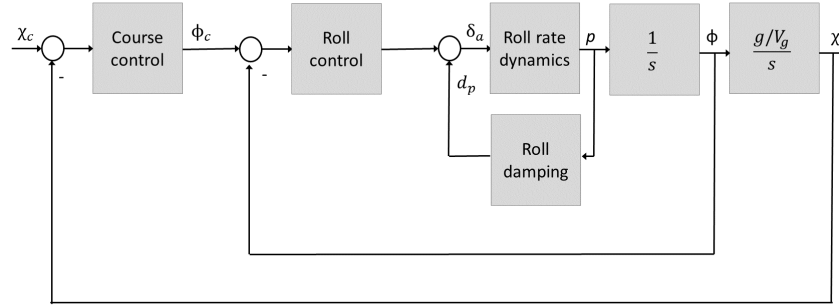


**Fig. 2** Lateral control loops for roll and course angles

- Course control and roll damping (aileron control input  $\delta_a$ )
- Sideslip hold (rudder control input  $\delta_r$ )

**Course control and roll damping:** The roll dynamics is illustrated in Figure 2, cf. Beard and McLain (2012) and the control loops are described below.

- The innermost loop is a damping of the roll dynamics that is typically not very well damped by the aerodynamics. This is implemented with a negative feedback from the pitch-rate  $p$  to the ailerons  $d_p = -k_{pp}p$ . For the design of the gain  $k_{pp}$  the roll rate dynamics are usually considered as first-order dynamic response from the aileron commands  $\delta_a$  to the roll rate  $p$ .
- The roll control is then usually a PI controller driven by the roll error  $\phi_c - \phi$  that considers the damped first-order roll rate response dynamics in addition to the integrator from roll rate  $p$  to roll angle  $\phi$ . The desired bandwidth and damping can be selected to shape the closed-loop transfer function from  $\phi_c$  to  $\phi$ . Integral action is used to compensate for wind disturbances as well as actuator/servo biases. A maximum roll angle saturation is usually implemented to ensure safe operation within a defined flight envelope.
- In a coordinated turn (side-slip angle  $\beta = 0$ ) the lateral acceleration is canceled out in the body coordinate frame. This corresponds to the course dynamics, Beard and McLain (2012)

$$\dot{\chi} = \frac{g}{V_g} \tan(\phi) \cos(\chi - \psi) \quad (1)$$

where  $g$  is acceleration of gravity,  $V_g$  is ground speed, and  $\chi_a = \chi - \psi$  is the difference between course angle  $\chi$  and heading angle  $\psi$ , known as the crab angle, see Figure 3. Usually  $\chi \approx \psi$  and  $\tan(\phi) \approx \phi$  so one can use the approximation  $\dot{\chi} = (g/V_g)\phi$ . Thus the dominating dynamics for the course control is the

integrator with gain  $g/V_g$  and the course controller can be implemented as a PI-controller driven by the course error  $\chi_c - \chi$ . Integral action is used to compensate for wind velocity disturbances.

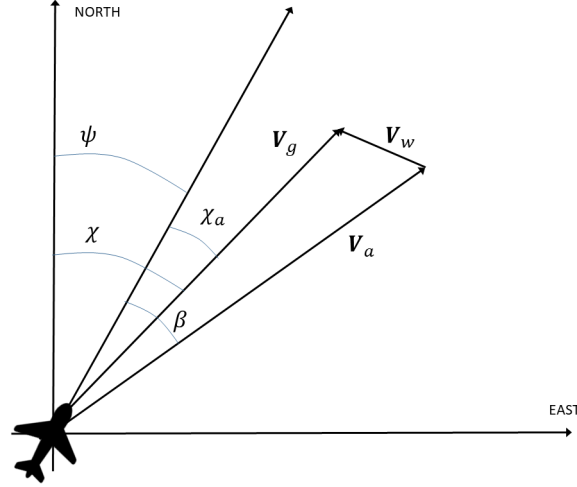


**Fig. 3** Projection onto horizontal plane with illustration of the heading angle  $\psi$ , course angle  $\chi$ , crab angle  $\chi_a$ , side slip angle  $\beta$ , air velocity vector  $\mathbf{V}_a$ , ground velocity vector  $\mathbf{V}_g$  and wind velocity vector  $\mathbf{V}_w$ .

**Sideslip hold:** On aircraft that have a rudder  $\delta_r$ , there is in addition usually a control loop that uses the rudder to compensate for nonzero side-slip angle.

- The dynamics from rudder to side-slip angle can be modeled as first-order dynamics, and a PI controller

$$\delta_r = -k_{p\beta}\beta - k_{i\beta}\int_0^t \beta d\tau \quad (2)$$

can be used to achieve the control objective  $\beta = 0$ . If the controller were to use only the rudder to initiate a turn in the air, the airplane would tend to skid to the outside of the curve. If the controller were to use only the ailerons to initiate a turn in the air, the airplane would tend to slip toward the lower wing.

**Path-following control:** The course command  $\chi_c$  that is the primary reference input to the lateral control system in Figure 2 is determined by the path following subsystem as shown in Figure 1. It is defined in different ways depending on the type of path segment that is currently being followed, where one usually distinguishes

between straight line path following and circular orbit path following at constant altitude. From the basic straight line and constant-altitude circular orbit path segments, one can synthesize Dubins paths which are time-optimal paths that combine circular and straight line segments, Dubins (1957); Beard and McLain (2012).

Let us first consider straight line path following. If there were no path errors involved, the course would be simply defined by the direction  $\chi_q$  from previous to next way points. In practice there is a lateral path error  $e_y$  due to winds and other disturbances. They can be measured as the projected horizontal plane distance between the UAV and the closest point on the path. It can be computed by orthogonal projections first to the horizontal plane at the level of the path, and then by another orthogonal projection to the path tangent. How quickly the UAV corrects for the error  $e_y$  is determined by a gain parameter  $k_y$  in the proportional guidance law, Beard and McLain (2012)

$$\chi_c = \chi_q - \chi_\infty \frac{2}{\pi} \tan^{-1}(k_y e_y) \quad (3)$$

where  $\chi_\infty$  is the desired angle (in general between 0 and 90 deg) at which the UAV should approach the desired path when it is far away. The gain parameter should consider the dynamic constraints of the UAV, in particular the maximum turning radius defined by the maximum roll angle and the ground speed. In order to avoid steady-state errors the proportional guidance law (3) can be modified to include integral action (PI guidance law), see Lekkas and Fossen (2014):

$$\chi_c = \chi_q - \tan^{-1}(k_{yp} e_y + k_{yi} y_{int}) \quad (4)$$

$$\dot{y}_{int} = \frac{V_g e_y}{\sqrt{\Delta^2 + (e_y + \kappa y_{int})^2}} \quad (5)$$

where  $\Delta > 0$  is the look-ahead distance,  $k_{yp} = 1/\Delta$ ,  $k_{yi} = k_{yp}\kappa$  and  $\kappa > 0$  is a tuning parameter.

Define a circular orbital path at constant altitude by

$$\mathbf{p} = \mathbf{p}_c + \lambda \rho \begin{pmatrix} \cos(\xi) \\ \sin(\xi) \\ 0 \end{pmatrix} \quad (6)$$

where  $\lambda \in \{-1, 1\}$  signifies counterclockwise and clockwise orbit, respectively,  $\rho$  is the desired radius,  $\xi$  is a phase angle variable for the UAV position along the orbit relative to North,  $\mathbf{p}_c$  is the desired center of the orbit, and  $\mathbf{p}$  is the desired position of the UAV. If there were no path errors, the desired course can be seen to be given by  $\xi + \lambda\pi/2$ . In order to compensate for the path error one can use the course command

$$\chi_c = \xi + \lambda \frac{\pi}{2} + \lambda \tan^{-1} \left( k_o \left( \frac{d - \rho}{\rho} \right) \right) \quad (7)$$

where  $d$  is the actual distance from the UAV position to the center  $\mathbf{p}_c$ , and  $k_o$  is a gain parameter that decides how quickly path error corrections are made, Beard and McLain (2012).

Care must be taken when computing  $\chi_q$  and  $\xi$  to avoid undesired effects related to integer multiples of  $2\pi$  that can arise in (3) and (7).

In some applications such as target tracking, the path following is not always based on way-points, but direct commands of course or course-rate from a high-level controller.

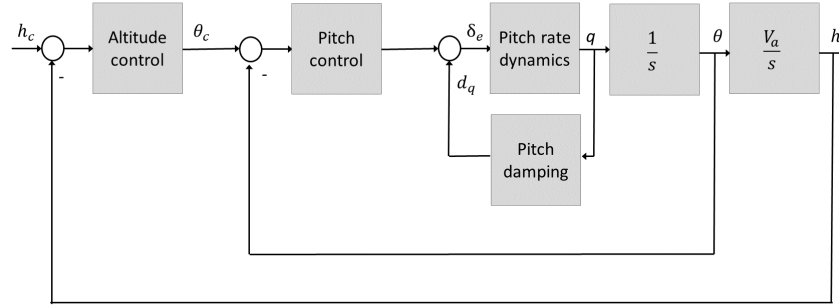


**Fig. 4** Longitudinal control loops for pitch and altitude.

### *Longitudinal guidance and control*

The decoupled longitudinal control loops are:

- Pitch and altitude control (elevator control input  $\delta_e$ )
- Speed control (throttle command / thrust control input  $\delta_t$ )

**Pitch and altitude control:** Typical longitudinal control loops for level flight at constant altitude are illustrated in Figure 4, cf. Beard and McLain (2012). Its control functions are designed as follows.

- The innermost control loop is the damping of the pitch dynamics by a feedback from the pitch rate  $q$  to the elevators,  $d_q = -k_{pq}q$ .
- In the pitch control loop, it is common to use a P controller driven by the pitch error  $\theta_c - \theta$ , and accept a steady-state errors due to wind disturbances in order to achieve highest possible bandwidth, Beard and McLain (2012).



- The effect of steady-state errors in the pitch control loop are compensated using integral action in the outer PI control loop, controlling altitude  $h$  and commanding a pitch set-point  $\theta_c$  to the pitch controller.

**Speed control:** Airspeed is usually controlled using a PI controller with feedback from airspeed error to the engine throttle command. This usually includes a feed-forward command given by the reference airspeed. During climb or decent, the altitude controller in Figure 4 can be replaced by a control of the flight path angle  $\gamma$ , see Figure 5. Alternatively, one might set the throttle command to preset values suitable for climb or descent, and control the pitch or flight path angle using the elevators.

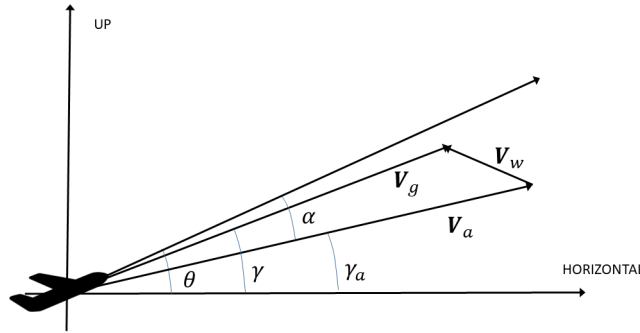


**Fig. 5** Projection onto vertical plane with illustration of the pitch angle  $\theta$ , flight path angle  $\gamma$ , air-referenced flight path angle  $\gamma_a$ , angle of attack  $\alpha$ , air velocity vector  $V_a$ , ground velocity vector  $V_g$  and wind velocity vector  $V_w$ .

Since the aerodynamic model parameters depend significantly on the airspeed  $V_a$ , the control parameters are usually gain-scheduled depending on the airspeed in order to achieve consistent performance over a range of airspeeds.

Instead of separating the airspeed and altitude control, an alternative is total energy control where the strong couplings between airspeed and altitude are considered jointly by a multivariate controller that controls the total and differential kinetic and potential energy compared to a reference using throttle and pitch commands, Lambregts (1983).

## Navigation

The common sensor configuration for small UAVs is summarized in Table 1. GNSS refers to global navigation satellite systems, such as GPS, which is used to measure both position and velocity in an Earth-fixed coordinate frame. From the GNSS velocity, it is possible to directly derive speed over ground  $V_g$ , course angle  $\chi$  and

flight path angle  $\gamma$ . The main limitation of the GNSS-based measurements is that they have relatively low update frequency (usually 1-10 Hz) and that position errors may be significant, i.e. 10 meters or more slowly drifting error in the altitude. For this reason, it is common to combine GNSS with inertial sensors (accelerometers and rate gyros) to achieve position and velocity estimates at higher sampling frequency and with less high-frequency noise, and also to use pressure-based altimeter for the vertical position. Note that the pressure-based altimeter may also have significant errors due to natural variations in atmospheric pressure.

**Table 1** Summary of UAV sensors and their primary function. AHRS refers to attitude and heading reference system.

Sensor	Primary function	Remarks
Accelerometers	Roll ( $\phi$ ) and pitch ( $\theta$ )	Also for inertial navigation and AHRS
Rate gyros	Angular rates $p, r, q$	Also for inertial navigation and AHRS
Pitot-static tube	Airspeed ( $V_a$ )	Measures dynamic pressure
Pressure altimeter	Altitude ( $h$ )	Measures static atmospheric pressure
GNSS	Ground position and velocity	Optional: Two-antenna GNSS for heading
Magnetometer	Heading ( $\psi$ )	Optional

A main challenge is that roll and pitch angles cannot be measured directly, but only indirectly by accelerometers and rate gyros. The kinematic model of the rigid body provides a model, Beard and McLain (2012),

$$\dot{\phi} = p + q \sin(\phi) \tan(\theta) + r \cos(\phi) \tan(\theta) \quad (8)$$

$$\dot{\theta} = q \cos(\phi) - r \sin(\phi) \quad (9)$$

that can be combined with a model of the accelerometer measurements (specific forces)  $(f_x, f_y, f_z)$  decomposed in the body-fixed coordinate frame

$$f_x = \dot{u} + qw - rv + g \sin(\theta) \quad (10)$$

$$f_y = \dot{v} + ru - pq - g \cos(\theta) \sin(\phi) \quad (11)$$

$$f_z = \dot{w} + pv - qu - g \cos(\theta) \cos(\phi) \quad (12)$$

where  $(u, v, w)$  are the components of the linear ground velocity of the UAV decomposed in the body-fixed coordinate frame, and  $p, q, r$  are the angular rates about the roll, pitch and yaw axes, respectively. Estimates are usually computed based on the above models using a nonlinear approximation to the Kalman-filter, e.g. Beard and McLain (2012); Groves (2013), or a nonlinear observer, e.g. Grip et al (2013); Bryne et al (2017). This estimator usually also includes estimation of rate gyro sensor biases and uses GNSS position and velocity measurements that are coupled with the attitude dynamics through a rotation matrix between the body-fixed and Earth-fixed coordinate frames, and the translational motion dynamics of the UAV. Moreover, the wind velocity  $\mathbf{V}_w$  can also be estimated using the same models by also including the measurement equation for the air speed ( $V_a$ ), Johansen et al (2015); Beard and

McLain (2012). This also enables estimation of the angle of attack ( $\alpha$ ) and side-slip ( $\beta$ ).

## Example of Applications

The primary application of fixed-wing UAVs is as a platform for payload sensors such as cameras and other imaging sensors. In such applications the path planning usually involves mapping or surveillance of a given geographic area. A pre-programmed mission plan is then usually defined by a sequence of way-points to cover a lawn mower pattern, or other relevant pattern, to search the area. Other applications involve tracking of targets of interest, where the UAV may be commanded to loiter over the target (circular orbit), the orbit parameters or way-points are updated dynamically in order to follow the target, or the course change is commanded directly from a target tracking guidance algorithm. Some flight modes would require high precision navigation and control, such as automatic landing (especially on moving platforms such as ships) and applications such as precision agriculture and inspection of power network infrastructure. In order to decouple the UAV's high-frequency motion from the payload sensor data, the payload sensors may be suspended in a gimbal or vibration damping arrangement.

## Future Direction for Research

The control design surveyed in this paper is a classical approach, with legacy from conventional flight control where the safety and comfort of passengers and crew is of primary concern. In a small UAV it might be of interest to define flight envelopes where the UAV is operating closer to the physical limits, allowing more agile maneuvers and increased the robustness to unsteady winds and turbulence. This means that nonlinear effects such as stall, actuator saturation and coupled dynamics needs to be considered in the control design, e.g. Girish et al (2015). Strongly nonlinear effects are also exhibited by hybrid fixed-wing UAVs that reconfigure propulsion for VTOL (vertical take-off and landing), Casau et al (2011), as well as UAVs that are designed for deep-stall landing, Mathisen et al (2016).

Functionality for detect-and-avoid is essential for safe operation of UAVs, in particular in airspace shared with conventional air traffic. Collision avoidance control strategies are needed, considering collaborative schemes based on traffic rules and negotiation of safe mitigation actions by the involved aircraft, Richards and How (2002); Radmanesh et al (2015). The dynamic performance constraints of the UAV may also be important to consider.

For operations beyond visual line-of-sight (BVLOS), the requirements for autonomy and safety increases. In particular, the redundancy, robustness and fault tolerance in navigation is an essential feature since navigation failure might trigger

safety mechanisms such as flight termination. An interesting future research direction is navigation when GNSS is not available, using visual odometry and SLAM techniques, Scaramuzza (2019); Chli (2019); Torres-González (2019), local radio navigation Fresk et al (2017); Gryte et al (2017) or phased-array radio antennas, Albrektsen et al (2018).

## References

- Albrektsen SM, Bryne TH, Johansen TA (2018) Phased array radio system aided inertial navigation for unmanned aerial systems. In: Proceedings IEEE Aerospace Conference, Big Sky
- Alexis K, Dang T, Mascarich F, Khattak S, Papachristos C (2019) Informative path planning for autonomous aerial robots. In: Encyclopedia of Robotics, Springer
- Beard RW, McLain TW (2012) Small unmanned aircraft - theory and practice. Princeton University Press
- Bryne TH, Hansen JM, Rogne RH, Sokolova N, Fossen TI, Johansen TA (2017) Nonlinear observers for integrated INS/GNSS navigation - implementation aspects. IEEE Control Systems Magazine 37(3):59 – 86
- Casau P, Cabecinhas D, Silvestre C (2011) Autonomous transition flight for a vertical take-off and landing aircraft. In: 50th IEEE Conference on Decision and Control and European Control Conference, pp 3974–3979
- Chli M (2019) Visual simultaneous localization and mapping. In: Encyclopedia of Robotics, Springer
- Dubins LE (1957) On curves of minimal length with a constraint on average curvature, and with prescribed initial and terminal positions and tangents. American Journal of Mathematics 79:497–516
- Fresk E, Ödmark K, Nikolakopoulos G (2017) Ultra wideband enabled inertial odometry for generic localization. In: Proc. 20th IFAC World Congress, Toulouse
- Girish CV, Frazzoli E, How JP, Hugh L (2015) Nonlinear flight control techniques for unmanned aerial vehicles. In: Valavanis K, Vachtsevanos G (eds) Handbook of Unmanned Aerial Vehicles, Springer, Dordrecht
- Grip HF, Fossen TI, Johansen TA, Saberi A (2013) Nonlinear observer for gnss-aided inertial navigation with quaternion-based attitude estimation. In: American Control Conference, Washington DC
- Groves PD (2013) Principles of GNSS, Inertial, and Multisensor Integrated Navigation Systems, second edition edn. Artech House
- Gryte K, Hansen JM, Johansen TA, Fossen TI (2017) Robust navigation of UAV using inertial sensors aided by UWB and RTK GPS. In: Proc. AIAA Guidance, Navigation, and Control Conference, p 1035
- Johansen TA, Fossen TI (2013) Control allocation - a survey. Automatica 49:1087–1103
- Johansen TA, Cristofaro A, Sørensen KL, Hansen JM, Fossen TI (2015) On estimation of wind velocity, angle-of-attack and sideslip angle of small UAVs using standard sensors. In: International Conference on Unmanned Aircraft Systems, Denver
- Lambregts AA (1983) Vertical flight path and speed control autopilot design using total energy principles. In: Proceedings of the AIAA Guidance and Control Conference, pp 559–569
- Lekkas A, Fossen TI (2014) Integral los path following for curved paths based on a monotone cubic hermite spline parametrization. IEEE Transactions on Control Systems Technology 22(6):2287–2301
- Mathisen S, Gryte K, Johansen TA, Fossen TI (2016) Non-linear model predictive control for longitudinal and lateral guidance of a small fixed-wing UAV in precision deep stall landing. In: AIAA Guidance, Navigation, and Control Conference, San Diego

- Maza I, Ollero A (2019) Cooperation of multiple aerial systems. In: Encyclopedia of Robotics, Springer
- Radmanesh M, Kumar M, Nemati A, Sarim M (2015) Dynamic optimal UAV trajectory planning in the national airspace system via mixed integer linear programming. Proceedings of the Institution of Mechanical Engineers, Part G: Journal of Aerospace Engineering 230:1668–1682
- Richards A, How JP (2002) Aircraft trajectory planning with collision avoidance using mixed integer linear programming. In: Proceedings of American control conference, pp 1936–1941
- Scaramuzza D (2019) Visual odometry of aerial robots. In: Encyclopedia of Robotics, Springer
- Torres-González A (2019) Range only simultaneous localization and mapping. In: Encyclopedia of Robotics, Springer
- Tsourdous A, White B, Shanmugavel M (2010) Cooperative path planning of unmanned aerial vehicles. John Wiley & Sons